PHYSICAL REVIEW B, VOLUME 63, 245328

Origin of band-*A* emission in diamond thin films

D. Takeuchi,*,† H. Watanabe,* S. Yamanaka,*,‡ and H. Okushi*
Research Center for Advanced Carbon Materials, National Institute of Advanced Industrial Science and Technology, 1-1-1 Higashi, Tsukuba 305-8565, Ibaraki, Japan

H. Sawada* and H. Ichinose*
Department of Material Science, The University of Tokyo 7-3-1 Hongo, Bunkyo-ku 113-8656, Tokyo, Japan

T. Sekiguchi*
Nanomaterials Laboratory, National Institute for Materials Science, 1-2-1 Sengen, Tsukuba 305-0047, Ibaraki, Japan

K. Kajimura*
Japan Society for the Promotion of Machine Industry, 3-5-8 Shiba-Koen, Minato-ku, Tokyo 105-0011, Japan
(Received 28 November 2000; published 8 June 2001)

By means of scanning cathodoluminescence (CL) measurements, high-resolution transmission electron microscopy (HRTEM), and electron energy loss spectroscopy (EELS), we have studied the origin of the band-*A* emission in homoepitaxial diamond thin films grown using microwave-plasma chemical vapor deposition (CVD). A broad luminescence peak at around 2.9 eV, the band-*A* emission, was observed in homoepitaxial diamond films with nonepitaxial crystallites (NC's), but not in the high-quality films without NC's. The scanning CL measurements showed that the band-*A* emission appeared only at NC sites. TEM revealed that the NC's contained defects such as dislocations and several types of grain boundary (GB). Further, HRTEM indicated that several types of incoherent GB existed within the NC's including five-, six-, and seven-member carbon atom rings. These were the same GB's as those in polycrystalline CVD diamond films that had sp^2-like structure of carbon atoms as indicated by the observation of the 1s-π^* signal in EELS. It is then reasonable to consider that, if sp^2-like structures behave as defects in the network of sp^3 structure of diamond, one possible origin of band-*A* emission might be the sp^2 defects in the GB's and dislocations. The band-*A* emission behavior in homoepitaxial CVD diamond films is the same as that in polycrystalline diamond films. The origin of the band-*A* emission generally observed in many kinds of CVD diamond is discussed relative to these results.

DOI: 10.1103/PhysRevB.63.245328 PACS number(s): 73.20.Hb, 61.72.Ff, 61.72.Mm, 78.60.Hk

I. INTRODUCTION

Diamond usually shows a broad emission peak at around 2.8–2.9 eV in cathodoluminescence (CL), which is the so called band-*A* emission. In many reported investigations, natural diamond and homoepitaxial single-crystal diamond films and polycrystalline diamond films deposited by chemical vapor deposition (CVD) have been used to study band *A*.[1–9] However, the diamond materials used in these investigations included high concentrations of many kinds of impurities and defects.[10] Because of many complicating factors, these imperfections of the specimens prevented us from previously investigating the origin of the band-*A* peak.

Recently we found that homoepitaxial diamond films grown using low CH_4/H_2 ratio ($<0.15\%$) conditions in microwave-plasma CVD show strong intrinsic excitonic emission (5.27 eV) at room temperature (RT),[11,12] and also their band-*A* emission (2.85–2.95 eV) in CL disappeared.[13,14] These homoepitaxial layers had atomically flat surfaces over entire substrate areas of dimensions 4 mm $\times$ 4 mm.[15] This allowed reliable fabrication of ideal Schottky junctions on these device grade films.[12,16]

When the homoepitaxial diamond films included nonepitaxial crystallites (NC's; denoted as UC's in our previous reports) due to higher CH_4/H_2 ratio conditions (0.15%–0.5%) during growth, scanning CL measurements showed that the band-*A* emission appeared only at NC sites. Other flat surface portions still showed intrinsic excitonic emission.[13,14] Therefore, it was clear that there was a correlation between the NC's and the band-*A* emission sites in the homoepitaxial diamond films.

In this work, the crystal structure and electronic states of the NC sites in single-crystal homoepitaxial diamond films have been investigated by means of scanning CL, high-resolution transmission electron microscopy (HRTEM), and electron energy loss spectroscopy (EELS).[17,18] An advanced CL measurement system with field emission scanning electron microscopy (FE-SEM) and focused ion beam (FIB) machining has enabled us to develop a direct approach to investigating the emission sites in cross section at sub micrometer scale. HRTEM and EELS have given us nanometer scale information. The origin of the band-*A* emission generally observed in many kinds of CVD diamond films is discussed based upon these results obtained from homoepitaxial films.

II. EXPERIMENT

Diamond growth was carried out using a microwave-plasma CVD reactor equipped with a temperature-controllable substrate holder employing a 50 kHz rf induc-

tion heating system. The system allowed us to control the substrate temperature and the microwave power independently. A stainless steel chamber wall was used in the system in order to avoid contamination of the deposited diamond films with silicon.[19]

The diamond films were deposited onto high-pressure and high-temperature synthesized *Ib* (001) diamond substrates of dimensions 4 mm×4 mm×0.3 mm. Diamond thin films were synthesized under 0.025% and 0.5% CH_4/H_2 ratios. Gas pressure, total gas flow rate, substrate temperature, and microwave power were 25 Torr, 400 SCCM (SCCM denotes cubic centimeters per minute at STP), 800° C, and 750 W, respectively. The purity of the CH_4 and H_2 gases was 99.999% and 99.99999%. Deposition duration was selected to get enough thickness for each measurement. The thickness of the high-quality homoepitaxial CVD diamond film without NC's was 0.2 μm obtained using a 0.025% CH_4/H_2 ratio for 42 h, and that of the homoepitaxial film with NC's was 2 μm obtained using a 0.5% CH_4/H_2 ratio for 6 h.[13] Misorientation angles of all the diamond substrates used in this work were measured by the x-ray rocking curve method employing the diamond (004) plane peak. The misorientation angles of all the substrates were found to be lower than 2°.[20]

After growing the homoepitaxial diamond thin films, optical microscopy, scanning electron microscopy, and field emission scanning electron microscopy (Hitachi S-4200T) were used to investigate the surface morphologies. Electronic states in the bulk regions were investigated by means of CL measurements. For the scanning CL system with conventional SEM, the accelerating voltage of the *e* beam was 10 kV or 30 kV while the beam current was kept at approximately 1 nA. Emission was detected at low temperatures (20 K and 60 K), or at room temperature using a charge-coupled device camera (Jovin Yvon, Spectra View-2D).[21] For the line scanning CL system with FE-SEM, the accelerating voltage of the *e* beam was 4 kV while the beam current was kept at approximately 1 nA. Emission was detected at RT. HRTEM (JEM-ARM1250) and EELS were used to analyze the structures of the CVD diamond films structures.[17,18] The samples for HRTEM observations were prepared by means of cleaving and thinning with FIB (FEI JFIB-2100) sputtering.

III. RESULTS

Figure 1 shows the CL spectra of homoepitaxial CVD diamond films grown under 0.5% and 0.025% CH_4/H_2 ratios. The inset pictures are optical microscope images of the film surfaces.[13,15] The CL measurements were carried out at 20 K with 10 kV acceleration of the *e* beam. With the of 0.5% CH_4/H_2 ratio, NC's and pyramidal hillocks (PH's) were observed in the smooth epitaxial region (ER), and the band-*A* emission of the homoepitaxial diamond film appeared at 2.883 eV. In our experiments, the band-*A* emission appeared in the range from 2.85 to 2.95 eV. The broadness of this line remained over the range from RT to 20 K as did the band-*A* emission observed from polycrystalline CVD diamond films. On the other hand, with a 0.025% CH_4/H_2 ratio, NC's and PH's disappeared, and the band-*A* emission also disappeared.[13] In this manner, we were able to use the homoepitaxial diamond films grown with a 0.5% CH_4/H_2 ratio to study the origin of the band-*A* emission.

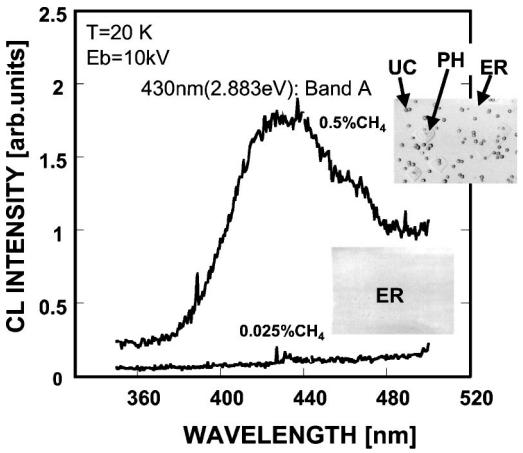

FIG. 1. CL spectra of homoepitaxial CVD diamond films grown under 0.5% and 0.025% CH_4/H_2 ratios. Inset is optical microscope images of the film surfaces. This CL measurement was carried out at 20 K with 10 kV acceleration of the *e* beam.

Figure 2(a) shows a SEM image of a homoepitaxial diamond film, and Figs. 2(I) and 2(II) show scanning CL images of the band-*A* emission and intrinsic excitonic emission lines at 60 K, respectively. The scan area shown is 80 μm^2. Labels 1 and 2 indicate the NC and PH, respectively. From these images, it was found that the line I (band-*A* emission) was observed at the NC sites, and the line II (excitonic emission) was present in the whole area except at the NC sites. In short, a complementary relationship in emission intensity was observed between lines I and II.[13,14] Several spotty patterns in the line I image in this figure were also observed in the smooth epitaxial region as marked with a dotted circle in these images. Our results indicate that there are embedded NC's in the film, which grew under conditions of a ratio of CH_4/H_2 above 0.15%.[13–15]

Figure 3 shows the FE-SEM images of the same NC. The image on the right is rotated 90° from the one on the left. The bottom of each figure shows the result of line scanning CL at RT. The horizontal axis is the position that corresponds to the white dotted line in the top FE-SEM images, while the vertical axis is the wavelength. The thickness of this NC was approximately 2 μm, while the sampling depth was 1 μm.[22] The figure illustrates that the band-*A* emission sites existed mainly inside the NC.[23]

Additionally we applied a different method to obtain CL results on cross sections of NC's in homoepitaxial diamond films as shown in Fig. 4. We cleaved a sample to obtain small pieces. Usually the samples were cleaved along their {111} faces, and had surface widths from 50 to 300 μm along the [110] direction. After selecting a suitable piece that included NC's on the (001) surface, one side of the NC was etched by means of FIB sputtering in order to observe the section inside. Sample surfaces were covered by deposited tungsten before FIB sputtering in order to avoid degrading the sample surface. Then a line scanning analysis of CL with FE-SEM was carried out within the cross section of the sample.

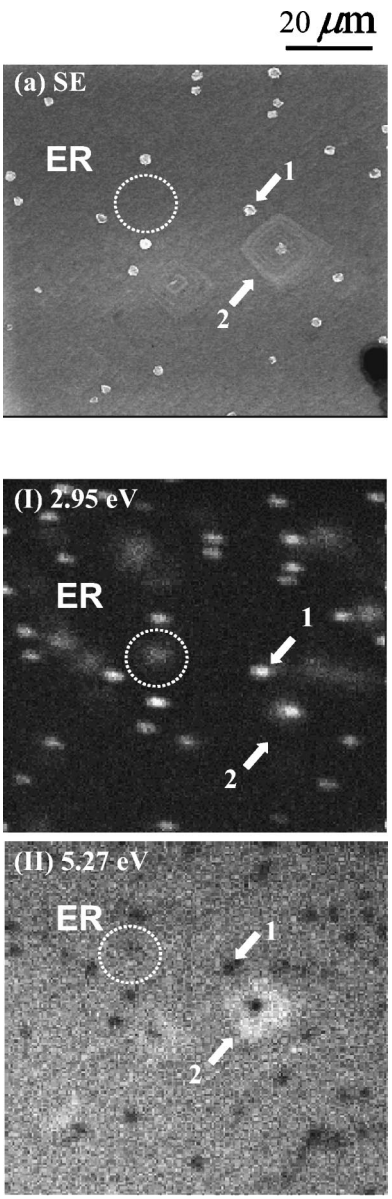

FIG. 2. (a) A SEM image of a diamond film, and (I) and (II) the scanning CL images of the band-*A* emission and excitonic emission lines at 60 K, respectively. The scanning area is 80 μm^2. Labels 1 and 2 indicate the NC and PH, respectively. Several spotty patterns in the line I images in this figure were also observed in the smooth epitaxial region (ER) as marked with a dotted circle in these images. Our results indicate that there are embedded NC's.

After the CL measurements, HRTEM was used to analyze the cross sectional structure of the same NC. The samples for HRTEM observations were prepared by thinning the opposite side of the NC by FIB sputtering again as shown in Fig. 4. The width of the slice of NC was from a few hundred to 2000 Å. An example of the sample is also shown in Fig. 4. We observed the cross sectional HRTEM images, and then compared them directly with the CL map.

We carried out line scanning CL measurements for a NC from top to bottom and made a map of the band-*A* emission by sampling the emission intensity at 430 nm wavelength as shown in Fig. 5. Figure 5(a) shows the cross stripes of scanning lines by FE-SEM, (b) the CL intensity map at 430 nm wavelength, and (c) the cross sectional TEM image. A pixel in Fig. 5(b) corresponds to 0.14 μm^2.

According to Figs. 5(a) and 5(b), the left top quarter of this NC showed the band-*A* emission, and the center of this area showed the strongest intensity. Comparing with Fig. 5(c), grain boundaries (GB's) and/or dislocations were observed around the band-*A* emission site.

Figure 6 shows HRTEM images of two GB's typically observed in NC's. These GB's are described using the coincidence site lattice model.[24] In this figure, two {111} $\Sigma 3$ are connected with {112} $\Sigma 3$ units, which include five-, six-, and seven-member rings of carbon atoms. According to Refs. 17 and 18, EELS of the same types of GB in a polycrystalline diamond film was successfully measured by a line subtraction process. {112} $\Sigma 3$ showed the 1s-π^* line, while {111} $\Sigma 3$ did not. This indicates that {112} $\Sigma 3$ has sp^2 states while {111} $\Sigma 3$, which is a stacking fault, does not. Thus, {111} $\Sigma 3$ is the so called coherent GB, and {112} $\Sigma 3$, is an incoherent GB.

Here we put the features of the GB's in order as shown in Table I. The GB's listed in the table were mainly observed in NC's and between a NC and the ER. The results from polycrystalline diamond films reported in Refs. 17 and 18 are also given. The EELS results marked † were observed only in polycrystalline films. We consider that such GB's at NC sites in our homoepitaxial diamond films were so short relative to those in polycrystalline films that the EELS intensity was too weak to detect. {111}/{115} $\Sigma 3$ was observed between NC and ER, showing the 1s-π^* line. In short, GB's can be classified into two types; one exhibiting the 1s-π^* line attributed to the sp^2-like structure of carbon atoms, and the other which does not.

IV. DISCUSSION

A number of models of the origin of band-*A* emission have been reported. The most widely used model for more than two decades, which is due to Dean,[4,25] is based on the donor-acceptor (DA) pair recombination mechanism. This DA pair model is based on randomly distributed boron as the acceptor. However, this model cannot be strictly applicable to band-*A* emission because undoped films with no trace of substitutional boron also clearly show the band-*A* emission.[4,7]

Based on both CL and TEM data, it is generaly accepted that the band-*A* emission can be attributed to lattice disorder such as dislocations.[2–8] But it has also been reported that not all dislocations are luminescent[1,2] nor has there been any correlation with the type of dislocation.[3]

Iyer *et al.* have suggested a vibronic (vibrational-electronic) model for the origin of band-*A* emission, and have simulated it with a semiempirical calculation.[26] They assumed dangling bonds in the dislocation core in diamond, and found that the dangling bonds reconstructed by forming a distorted σ bond between the adjacent atoms along the dislocations. Their results showed good agreement with the experimental data; however, they needed a very large contribution of the electron-phonon coupling by means of a high *S*

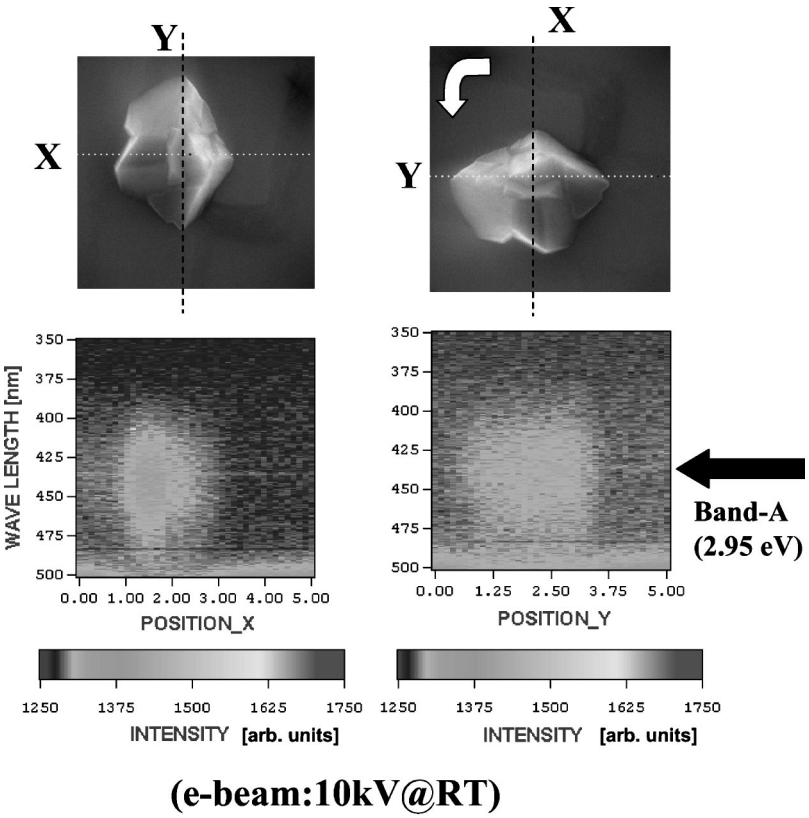

FIG. 3. FE-SEM images of the same NC. The right image is rotated 90° the left. The lower panels correspond to the CL maps. The horizontal axis is the position compared to that corresponds to the white dotted line in the top FE-SEM images, while the vertical axis is wavelength.

parameter (the Huang-Rhys factor),[4] and the basic structural model of the dislocation core has not yet been revealed in any experiments.

Homoepitaxial diamond films have been used for studying emission lines of diamond because of the ease of obtaining single-crystalline films.[9] These films have also showed band-*A* emission in CL. However, they were grown not only with CH_4/H_2 gas, which consists only of carbon and hydrogen, but also with other carbon sources containing oxygen (e.g., carbon monoxide) and/or impurity gases such as oxygen, diborane, and so on, in order to get smooth surfaces at high growth rates. In short, these specimens included not only dislocations but also impurities that complicate the study of the origin of the band-*A* emission. The band-*A* emission was observed inhomogeneously, and it has been difficult to determine its origin in the films.

We have clearly observed a complementary relationship between the intensity of the band-*A* emission and that of the free exciton as shown in Fig. 2 from our homoepitaxial diamond films.[12,14] The excitonic emission is intrinsic emission from diamond, and this emission shows the good quality of the diamond. The ER region, where homogeneously distributed sites of excitonic emission were observed in plane view, represents the perfect crystal perfection, and clearly we can identify the band-*A* emission only at NC sites. Consequently, these samples are appropriate specimens to discuss the origin of band-*A* emission in homoepitaxial diamond films.[13,14,23]

As shown in Fig. 5, there were defects in a NC, and it was clearly confirmed that the band-*A* emission of our homoepitaxial CVD diamond films was correlated with such structural defects as dislocations and GB's.

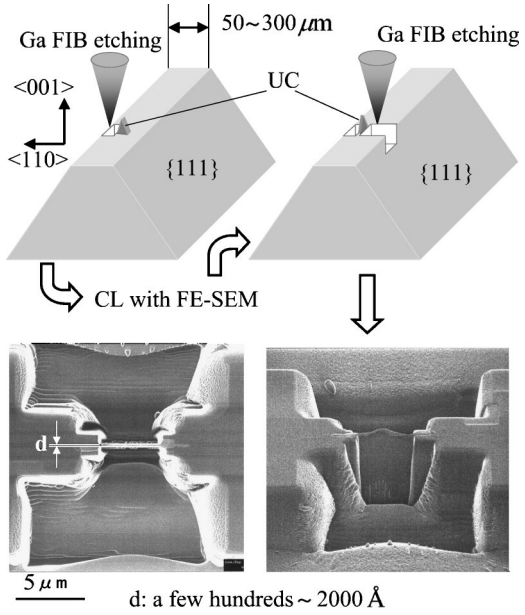

FIG. 4. A different method to obtain CL results on cross sections of NC's. First, we cleaved a sample and obtained small pieces. Second, we selected a suitable piece that included NC's on the (001) surface, and one side of a NC was etched by means of FIB sputtering to observe the inside section. Sample surfaces were covered with tungsten deposits before FIB sputtering to avoid degrading the sample surface. Then a line scanning analysis of CL with FE-SEM was carried out on a cross section of the sample.

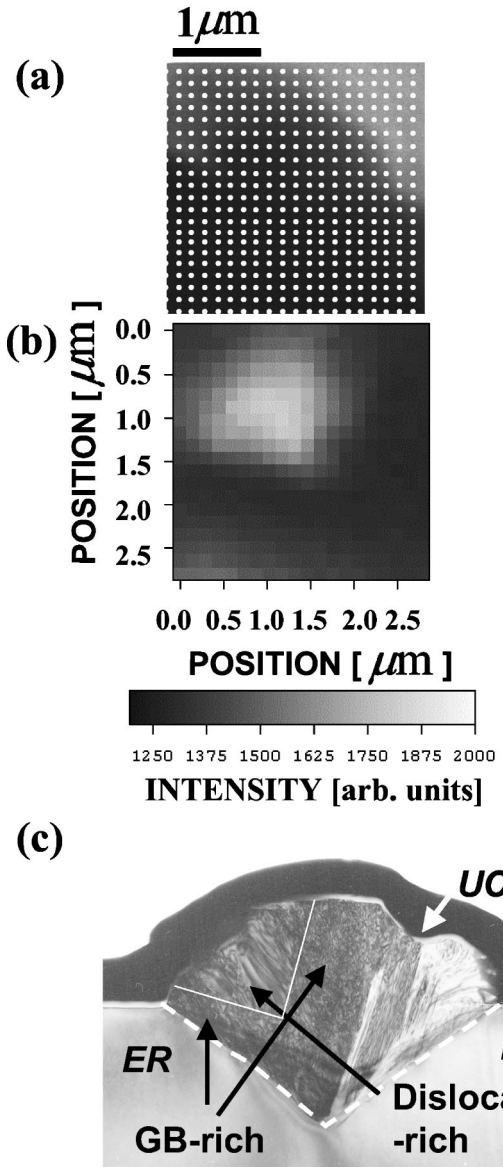

FIG. 5. (a) An example of scanning CL measurement of a NC in cross section (cross stripes), (b) the map of the band-*A* emission corresponding to (a) by sampling the emission intensity at 430 nm wavelength, and (c) the TEM image of the same area.

We observed many {111} $\Sigma 3$, which are stacking faults and coherent GB's, and short {112} $\Sigma 3$ predominantly as members of incoherent GB's in NC's. These incoherent GB's also existed in polycrystalline diamond films which had 1s-π^* lines in EELS as shown in Table I.[17,18] The existence of the 1s-π^* line in EELS is consistent with the crystallographic assignments of the incoherent GB's, in short, they include five-, six- and seven-member rings of carbon atoms, and indicate the presence of sp^2-like carbon atom structures.[17,18]

The structural unit of {112} $\Sigma 3$ in homoepitaxial diamond films is the same as that in polycrystalline CVD diamond films. The short {112} $\Sigma 3$ predominantly observed at NC sites in our homoepitaxial diamond films did not show the 1s-π^* line in EELS, as shown in Table I. However, we

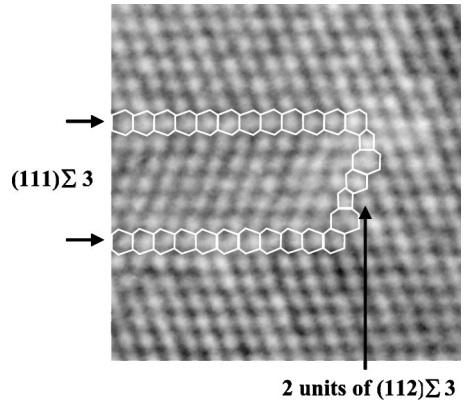

FIG. 6. The cross sectional HRTEM images of two GBs typically observed in NC's. These GB's are denoted with the coincidence site lattice (CSL) model. In this figure, two {111} $\Sigma 3$ are connected with {112} $\Sigma 3$, which included five-, six-, and seven-member rings of carbon atoms.

suspect that the {112} $\Sigma 3$ at the NC sites in our homoepitaxial diamond films were so short relative to those in polycrystalline films that the EELS intensity was too weak to allow detection of the 1s-π^* line.

As shown in Fig. 1, the band-*A* emission in our films showed broad spectra at 20 K. This behavior of the emission at low temperature is the same as that of the band-*A* emission in polycrystalline CVD diamond films. The band-*A* emission from both our homoepitaxial diamond films and polycrystalline diamond films is the same in general, and the same defect structures are also observed. Thus, the origin of the band-*A* emission generally observed in many kinds of CVD diamond can be discussed as follows.

The unit defects are typically sp^2-like structures. When the sp^2 states are based on the π-bond network, as in graphite, the π-bond network has no band gap and no localized states such as band-*A* within the band gap. However, it is reasonable to consider that, if the sp^2-like structures behave as defects within the sp^3 network of carbon atoms, they form localized states as midgap states. A preliminary computa-

TABLE I. Features of the GB's mainly observed in CVD diamond films. All GB's except {111}/{115} $\Sigma 3$ are observed at the NC sites in our homoepitaxial diamond films; and also in the polycrystalline films (denoted as ''poly'') as reported in Refs. 17 and 18. These show not only the 1s-σ^* line but also the 1s-π^* line in EELS. The EELS results marked (†) were observed only in polycrystalline films. We consider that such GB's at NC sites in the homoepitaxial diamond films were so much shorter than those in polycrystalline films that the EELS intensity was too weak to detect. {111}/{115} $\Sigma 3$ was observed between NC and ER in the homoepitaxial films, which showed the 1s-π^* line. In short, GB's are classfied into two types; one has the 1s-π^* line which is attributed to the sp^2-like structure of carbon atoms, and the other does not.

GB	{111}$\Sigma 3$	{112}$\Sigma 3$	{122}$\Sigma 3$	{114}$\Sigma 9$	{111}/{115}$\Sigma 3$
Site	NC, poly	NC, poly	NC, poly	NC, poly	NC/ER
EELS	1s-σ^*	1s-σ^*	1s-σ^*	1s-σ^*	1s-σ^*
		1s-π^* (†)		1s-π^* (†)	1s-π^*

tional result also indicated that the π bonds in incoherent GB's were unstable and sp^2 defects in the network of sp^3 structure of diamond showed midgap states.[27,28]

This suggests that the sp^2 defects should be taken into account in the model of the origin of band-*A* emission based on the experimental results. The vibronic model reported by Iyer *et al*. has strong advantages for considering the broadening features of the band-*A* emission; however, their defect model is based on σ bonds only. There are possibilities of reducing the excess contribution of the electron-phonon coupling when the computation is started by means of the sp^2 defects in dislocations and/or GB's.[4,26]

If we classify dislocations and GB's into two types depending upon whether the defects include sp^2-like structure, the observations that not all dislocations are luminescent[1,2] and that there is no correlation with the type of dislocation[3] can be understood.

Between the NC and the ER, we found many types of GB and dislocation, and very complicated structures were present inside NC's.[13] In the case of {111}/{115} $\Sigma 3$ observed at the NC/ER boundary, this showed the 1s-π^* line in EELS, as shown in Table I, but this GB did not correspond to a site of band-*A* emission. Figures 3 and 5 show that the band-*A* emission sites existed mainly inside the NC.[23] We speculate that there are not only band-*A* emission sites between NC and ER, but also nonradiative centers around this boundary. Thus, CL of the band-*A* emission was masked by the nonradiative centers, and became invisible at this boundary.

Our results above associate the structural origin of the band-*A* emission in diamond with fine structural defects on the nanometerscale. They indicate that we need to take into account the sp^2 defects in the network of sp^3 structure of diamond at dislocations and incoherent GB's as origin of the band-*A* emission. The density, impurity assignments, and broadening mechanisms should be studied in subsequent investigtations.

V. CONCLUSION

The origin of the band-*A* emission from homoepitaxial diamond films grown by microwave-plasma chemical vapor deposition was investigated by means of scanning cathodoluminescence using conventional scanning electron microscopy, line scanning CL using field emission SEM, high-resolution transmission electron microscopy, and electron energy loss spectroscopy. A broad luminescence peak at around 2.9 eV, which is the so-called band-*A* emission, was observed in homoepitaxial diamond films with nonepitaxial crystallites but not in high-quality films without NC's. It was shown that incoherent grain boundaries such as {112} $\Sigma 3$ and dislocations were located inside the NC's where the band-*A* emission was observed. The same {112} $\Sigma 3$ also existed in polycrystalline CVD diamond films. It was reported that {112} $\Sigma 3$ in polycrystalline films showed the 1s-π^* line in EELS, which is attributed to the sp^2-like structure of carbon atoms. These experimental results indicate that the band-*A* emission in homoepitaxial films can be attributed to sp^2 defects in the network of sp^3 structures of diamond at incoherent grain boundaries and/or dislocations. Since the band-*A* emission behavior in homoepitaxial CVD diamond films was the same as that in polycrystalline films, this suggestion all takes into account the sp^2 defects in a model of the origin of band-*A* emission based on all the experimental results.

*Also at CREST, JST (Japan Science and Technology Corporation).

†Author to whom correspondence should be addressed. Email address: d.takeuchi@aist.go.jp

‡Present address: Tsukuba Research Laboratory, Sumitomo Chemical Co., Ltd., 6 Kitahara, Tsukuba, 300-3294 Ibaraki, Japan.

[1] I. Kiflawi and A.R. Lang, Philos. Mag. **30**, 219 (1974).

[2] S.J. Pennycook, L.M. Brown, and A.J. Craven, Philos. Mag. A **41**, 589 (1980).

[3] N. Yamamoto, J.C.H. Spence, and D. Fathy, Philos. Mag. B **49**, 609 (1984).

[4] J. Walker, Rep. Prog. Phys. **42**, 1605 (1979).

[5] H. Kawarada, Y. Yokota, Y. Mori, K. Nishimura, and A. Hiraki, J. Appl. Phys. **67**, 983 (1990).

[6] R.J. Graham, T.D. Moustakas, and M.M. Disko, J. Appl. Phys. **69**, 3212 (1991).

[7] J. Ruan, K. Kobashi, and W.J. Choyke, Appl. Phys. Lett. **60**, 3138 (1992).

[8] M. Marinelli, A. Hatta, T. Ito, A. Hiraki, and T. Nishino, Appl. Phys. Lett. **68**, 1631 (1996).

[9] S. Katsumata, Jpn. J. Appl. Phys., Part 1 **31**, 3594 (1992).

[10] For example, see *Diamond: Electronic Properties and Applications*, edited by L.S. Pan and D.R. Kania (Kluwer, Boston, 1995), Chap. 3, p. 61; P.K. Bachmann, D. Leers, and H. Lydtin, Diamond Relat. Mater. **1**, 1 (1991).

[11] P.J. Dean, E.C. Lightowlers, and D.R. Wight, Phys. Rev. A **140**, A352 (1965).

[12] H. Watanabe, K. Hayashi, D. Takeuchi, S. Yamanaka, T. Sekiguchi, H. Okushi, and K. Kajimura, Appl. Phys. Lett. **73**, 981 (1998).

[13] D. Takeuchi, H. Watanabe, S. Yamanaka, H. Okushi, and K. Kajimura Phys. Status Solidi A **174**, 101 (1999).

[14] H. Watanabe, D. Takeuchi, H. Okushi, K. Kajimura, and T. Sekiguchi, Solid State Phenom. **63/64**, 489 (1998).

[15] H. Watanabe, D. Takeuchi, S. Yamanaka, K. Kajimura, H. Okushi, and T. Sekiguchi, Diamond Relat. Mater. **8**, 1272 (1999).

[16] H. Umezawa, K. Tsugawa, S. Yamanaka, D. Takeuchi, H. Okushi, and H. Kawarada, Jpn. J. Appl. Phys., Part 2 **38**, L1222 (1999).

[17] H. Ichinose and M. Nakanose, in *Proceedings of the 6th NIRIM International Symposium on Advanced Materials (ISAM '99), Tsukuba, Japan, 1999*, edited by Y. Bando, M. Akaishi, H. Kanda, Y. Matsui, T. Kobayashi, K. Watanabe, K. Seki, and N. Yamashita (NIRIM, Tsukuba, 1999), p. 31.

[18] H. Ichinose and M. Nakanose, Thin Solid Films **319**, 87 (1998).

[19] K. Hayashi, S. Yamanaka, H. Okushi, and K. Kajimura, in *Diamond for Electronic Applications*, edited by D. Dreifus, A. Collins, C. Beetz, T. Humphreys, K. Das, and P. Pehrsson, MRS Symposia Proceedings Mater. Res. Soc. Symp. Proc. **416** (Ma-

terials Research Society, Pittsburgh, 1996), p. 217.
[20] D. Takeuchi, H. Watanabe, S. Yamanaka, H. Okushi, and K. Kajimura, Diamond Relat. Mater. **9**, 231 (2000).
[21] T. Sekiguchi and K. Sumino, Rev. Sci. Instrum. **66**, 4277 (1995).
[22] K. Kanaya and S. Okayama, J. Phys. D **5**, 43 (1972).
[23] D. Takeuchi, H. Watanabe, S. Yamanaka, H. Okushi, and K. Kajimura, in *Optical Microstructural Characterization of Semiconductors*, edited by M.S. Ünlü, J. Pifueras, N.M. Kalkhoran, and T. Sekiguchi, MRS Symposia Proceedings No. 588 (Materials Research Society, Pittsburgh, 2000), p. 87.
[24] *Grain Boundary Structure and Properties*, edited by G. A. Chadwick and D. A. Smith (Academic, London, 1976), p. 140.
[25] P.J. Dean, Phys. Rev. **139**, A588 (1965).
[26] S.B. Iyer, G. Ananthakrishna, B.M. Arora, and J. Chandrasekhar, Phys. Rev. B **55**, 4093 (1997).
[27] M. Kohyama, H. Ichinose, Y. Ishida, and M. Nakanose, Mater. Sci. Forum **207-209**, 261 (1996).
[28] M. Kohyama, H. Ichinose, Y. Zhang, Y. Ishida, and M. Nakanose, in *Proceedings of JIMIS-8, the Interface Science and Materials Interconnection, 1996*, edited by Y. Ishida, M. Morita, T. Suga, H. Ichinose, O. Ohashi, and J. Echigoya (JIM, Sendai, 1996), p. 367.